Distribution and Chemical Speciation of Arsenic in Ancient Human Hair Using Synchrotron Radiation

Ioanna Kakoulli,*[,†,‡] Sergey V. Prikhodko,[†] Christian Fischer,[†,‡] Marianne Cilluffo,[§] Mauricio Uribe,[∥] Hans A. Bechtel,[⊥] Sirine C. Fakra,[⊥] and Matthew A. Marcus[⊥]

[†]Materials Science and Engineering Department, University of California Los Angeles, PO Box 951595, Engineering V, Los Angeles, CA 90095-1595, United States

[‡]Cotsen Institute of Archaeology, University of California Los Angeles, A210 Fowler Building, Los Angeles, CA 90095-1510, United States

[§]Department of Integrative Biology and Physiology, 1031 Terasaki Life Sciences Building, PO Box 957239, University of California Los Angeles, CA 90095-7230, United States

[∥]Facultad de Ciencias Sociales de la Universidad de Chile, Av. Capitán Ignacio Carrera Pinto N°1045, Ñuñoa, Santiago de Chile, Chile

[⊥]Advanced Light Source, Lawrence Berkeley National Laboratory, 1 Cyclotron Road, MS 6-2100, Berkeley, CA 94720-8226, United States

Ⓢ Supporting Information

ABSTRACT: Pre-Columbian populations that inhabited the Tarapacá mid river valley in the Atacama Desert in Chile during the Middle Horizon and Late Intermediate Period (AD 500−1450) show patterns of chronic poisoning due to exposure to geogenic arsenic. Exposure of these people to arsenic was assessed using synchrotron-based elemental X-ray fluorescence mapping, X-ray absorption spectroscopy, X-ray diffraction and Fourier transform infrared spectromicroscopy measurements on ancient human hair. These combined techniques of high sensitivity and specificity enabled the discrimination between endogenous and exogenous processes that has been an analytical challenge for archeological studies and criminal investigations in which hair is used as a proxy of premortem metabolism. The high concentration of arsenic mainly in the form of inorganic As(III) and As(V) detected in the hair suggests chronic arsenicism through ingestion of As-polluted water rather than external contamination by the deposition of heavy metals due to metallophilic soil microbes or diffusion of arsenic from the soil. A decrease in arsenic concentration from the proximal to the distal end of the hair shaft analyzed may indicate a change in the diet due to mobility, though chemical or microbiologically induced processes during burial cannot be entirely ruled out.
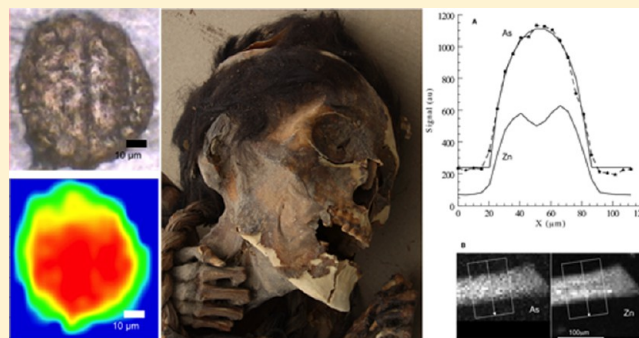
Ⓗuman hair is a widely accepted biomonitor in toxicology.[1,2] The chemical and physical attributes that provide hair with its robust structure facilitate its survival in adverse environmental conditions, while its biological formation and constant growth-rate (roughly 1 cm per month) make it useful as a biosensor of recent life history.[3] Bone and other tissues change throughout life, generating an average biogenic response over the remodeling timeframe. In contrast, once hair is keratinized, it no longer remodels and therefore offers superior chronological resolution.[3] In chronic exposure to toxic environments, hair analysis can therefore provide a longitudinal time-resolved signal.[4] Furthermore, arsenic and other toxic elements can be transported through the bloodstream to the hair fiber. The α-keratin in hair contains abundant thiol groups in its cysteine residues, which readily react with arsenic. Thus, the concentration of As in hair is much higher

than in other human biological tissues.[5,6] Consequently, owing to its intrinsic properties, hair provides an excellent bioresource in forensics and biological archeology.

Previous studies on hair analysis combined with paleopathological investigations of ancient pre-Columbian populations in northern Chile, from the Chinchorro culture to the Incas,[7−11] have indicated high levels of arsenic in both highland and coastal people, most likely as a result of long exposure to geogenic toxic contaminants through volcanism and weathering of arsenic-containing geological formations.[5,8−15] However, discriminating endogenous arsenic in hair (by ingestion) from external contamination has not always been possible and

remains an analytical challenge.[5,16] This is particularly true for archeological and historic hair that undergoes diagenetic alterations during burial[17] or subsequent conservation treatments involving the application of heavy metals as pesticides.[4,16,18] Combined analytical methods enabling the detection, spatial distribution, and speciation of arsenic on the same hair while requiring minimal sample preparation, offer a holistic approach for assessing As-exposure and discriminating between endogenous and exogenous processes.[4]

■ EXPERIMENTAL SECTION

Here we report synchrotron-based X-ray and Fourier transform infrared spectromicroscopy, field emission gun (FEG) variable pressure scanning electron microscopy (VPSEM), and energy dispersive X-ray spectroscopy (EDS) measurements, testing the hypothesis of arsenicism (chronic arsenic poisoning) among ancient populations in northern Chile.[4,8−10,12,16] μXRF mapping was first performed to obtain elemental distribution maps on the samples. Specific spots of interest were then selected on which to perform μXANES for chemical speciation and μXRD for identification of minerals. Complementary analyses on hair transverse thin sections (5 μm) were performed using synchrotron-based Fourier transform infrared (SR-μFTIR) spectroscopy. By combining the synchrotron techniques with FEGVPSEM-EDS, in situ submicrometer morphological characterization and topographic mapping were achieved with simultaneous spatially resolved elemental identification of the major and minor elements at the surface and subsurface of the hair, allowing accurate correlations with the synchrotron-based analytical data. Owing to the variable pressure capabilities of the FEGVPSEM, these insulating samples were analyzed without the need of any coating while maintaining the physical and chemical integrity and attributes of the specimens. We analyzed scalp hair from a 1000 to 1500-year-old mummy (Figure 1A) recovered from TR40-A, a pre-
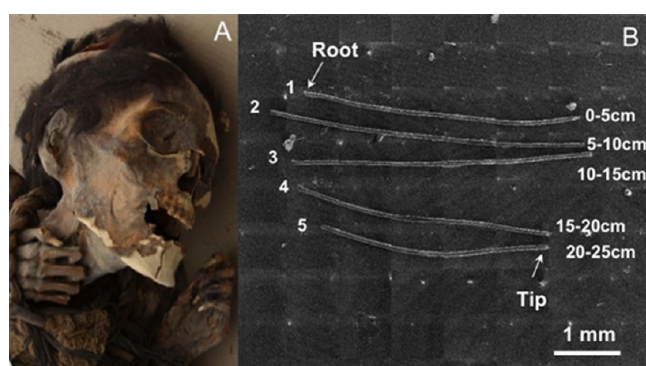

Figure 1. (A) Mummy bundle (Locus 9) from the TR40-A cemetery in the Tarapacá Valley in northern Chile. (B) Five hair segments from this mummy (∼4−5 mm each), cut along the entire length of a hair shaft at 5 cm intervals from the root (proximal end) to the tip (distal end). Photo of mummy 2008, Tarapacá Valley Archaeological Project, Ioanna Kakoulli.

Columbian cemetery in the Tarapacá Valley in 2005 and kept in an archival-quality storage facility. To characterize arsenic and other trace elements on the surface and inside the hair, μXRF elemental distribution maps were obtained on large areas (several mm) from five longitudinal segments along the entire hair length, approximately 25 cm from the root (proximal end) to the tip (distal end) (Figure 1B). For each area mapped, the

relative transverse profile distribution of arsenic was deduced by comparison to a theoretical model, taking into consideration the cylindrical geometry of the hair (see section 3.2 of the Supporting Information). The arsenic oxidation state was determined using As K-edge μXANES, while μXRD measurements combined with VPSEM-EDS phase maps were used to identify mineralogical phases associated with the burial soil. Complementary analyses on hair transverse thin sections (5 μm) to assess the degree of preservation of the hair were performed using μFTIR spectromicroscopy.

The analytical protocol followed in this study has several advantages over other conventional methods employed for arsenic-exposure studies, particularly for archeological and historical hair samples.[9,10,18,19] Since the use of synchrotron-based μFTIR, μXRF, and μXANES does not require elaborate sample preparation or extraction methods as in the case of chromatographic techniques,[5] the risk of chemical changes[20] during analysis within the sample is minimized when carefully monitored. In addition, the variable pressure capabilities of the FEGVPSEM enable the analysis of these insulating samples without the need of any conductive coating maintaining their physicochemical integrity. This further allows the reuse of the samples for subsequent analyses. In this research, the combination of these virtually nondestructive techniques allowed morphological and elemental spatially resolved characterization and chemical speciation in the same regions of the hair.

■ RESULTS AND DISCUSSION

Micromorphological characterization of the untreated hair segments using VPSEM indicated at first that the hair was well-preserved with evidence of well-maintained nits and underwent little taphonomic change (Figure 2).

SR-FTIR spectromicroscopy on 5 μm transverse sections (Figure 3), however, showed partial delipidization of the internal structure primarily affecting the lipids in the cortex, most likely as a result of postdepositional processes and microbial activity.[21,22] The degradation of the lipids backbone in the cortex was evidenced by the decrease in the ratio
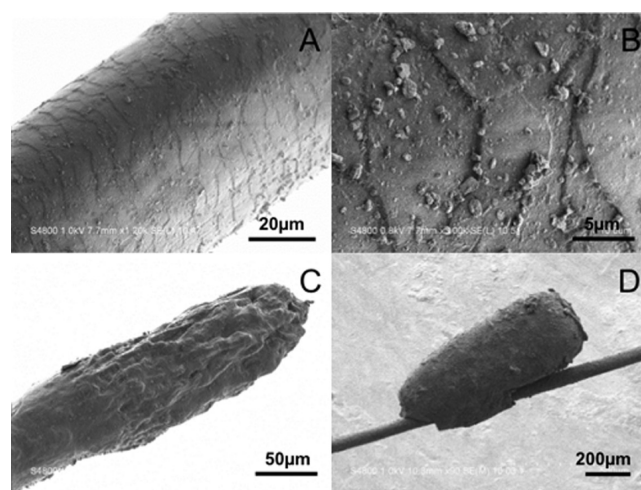

Figure 2. FEGVPSEM micrographs showing the intact preservation of the external morphology of the hair, clearly showing the imbricate scale pattern of (A and B) the cuticle and (C) a club-shaped root (proximal end). Lice infested this mummy and (D) a well-preserved nit is visible on this hair strand.
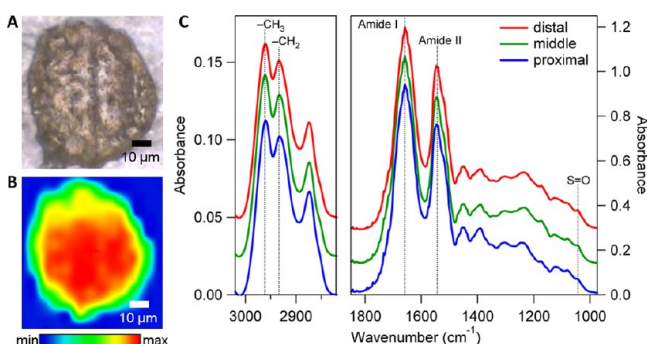
Figure 3. Transverse section of hair from (A) the middle of the shaft and identification and spatial distribution of the absorption band at ∼1660 cm^{-1} (Amide I), characteristic of (B) proteins. (C) FT-IR spectra from the proximal (blue), middle (green), and distal (red) end of the hair. All three spectra show absorption at ∼1040 cm^{-1} corresponding to the formation of cysteic acid as a result of oxidative damage to the hair. The spectra also show vibrational bands for amide I and II and −CH$_3$ and −CH$_2$ bands, characteristic of proteins and lipids, respectively.

between the asymmetric CH$_3$ and CH$_2$ stretch at ∼2960 cm^{-1} and ∼2930 cm^{-1} respectively. This ratio is similar among all hair segments (Figure 3C) and therefore excludes preferential oxidation along the length of the hair. This is further supported by evidence of consistent oxidative damage[23] at the proximal, middle, and distal end with the appearance of an absorption band at 1040 cm^{-1}, characteristic of the formation of cysteic acid (Figure 3C).

Speciation analysis of sulfur on the hair segments using S K-edge μXANES revealed mostly the presence of organic sulfur associated with structural proteins as well as inorganic sulfur in the form of sulfides and sulfates. EDS measurements on the unwashed hair cuticle showed the presence of S, K, Ca, Cl, Fe, Si, and Na, while μXRF also identified traces of Zn, As, and Ti. Soil data using a portable XRF (above Z = 13, due to the detection limit of pXRF) compared to the major and minor elements identified with the EDS. In addition, traces of arsenic (∼30 ppm) untraceable by EDS were also detected.

Additional measurements using EDS elemental maps combined with μXRF, μXANES, and μXRD data allowed the identification and mapping of particular salts and minerals attached to the hair cuticle, such as halite, pyrite, pyrrhotite, and quartz. These results are consistent with XRF and XRD data of the burial enveloping soil, pointing to a relatively immature sandy soil consisting of quartz, feldspars, and rock fragments with minor contributions from clay and iron-rich minerals. The salts identified in the soil are responsible for the relatively good preservation of human hair and human tissues and are often found in association with caliche, a characteristic deposit of the Atacama Desert that reflects its hyperaridity and the influence of a dense coastal fog known as camanchaca.[24]

μXRF mapping of arsenic at an incident energy below the Pb L$_3$-edge showed As in all five hair segments analyzed (Figure 4), with at least 150 ppm of total arsenic concentration in the hair matrix (see section 3.1 of the Supporting Information).

This concentration is 2 orders of magnitude greater than normal human levels in unexposed individuals estimated to less than 1 ppm in hair,[5,25] which was also confirmed by the undetectable arsenic in the control sample (of modern hair from an individual who has never been exposed to arsenic contaminated environments) (Figure 5).
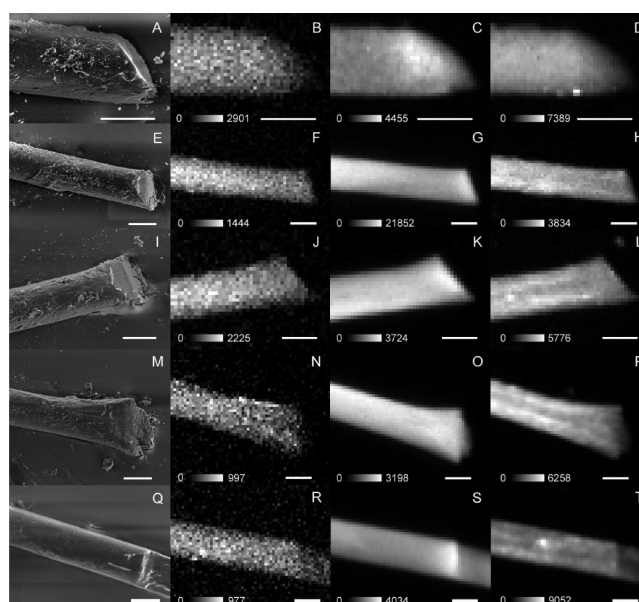

Figure 4. FEGVPSEM micrographs (A, E, I, M, Q) showing the external morphology of the hair and soil debris on five segments 1 to 5 from top to bottom (see also Figure1B). Corresponding μXRF maps of arsenic (B, F, J, N, and R), sulfur (C, G, K, O, and S), and zinc (D, H, L, P, and T) on the same hair segment locations (see the Supporting Information). A uniform radial distribution of arsenic, rather than coating the surface can be observed. Intensity scale bars show XRF counts in arbitrary units. Scale bars: 50 μm.
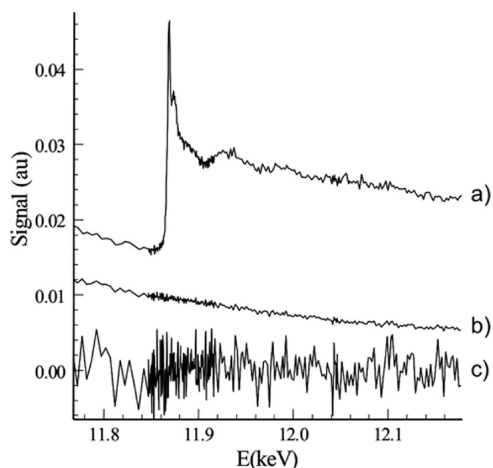

Figure 5. Average as K-edge μXANES spectra of (a) mummy hair segment 3 compared to (b) modern hair showing that modern hair has no detectable As. (c) Signal from the modern hair with a cubic polynomial subtracted off and multiplied by 10, to demonstrate the lack of an edge jump. All spectra are displayed on the same vertical scale.

Although the qualitative arsenic distribution appears higher closer to the center in all hair segments (Figure 4, B, F, J, N, and R), the distribution is consistent with a uniform concentration because the maximum thickness is at the midpoint of the cylindrically shaped hair. A lineout for arsenic profile in hair segment 3 (Figure 6) shows a good fit to the simple model of a uniform cylinder. Zn on the other hand (Figure 4D, H, L, P, and T and Figure 6) (see section 3.2 of the Supporting Information), an element that is mainly associated with diet and the third most abundant element in the hair of
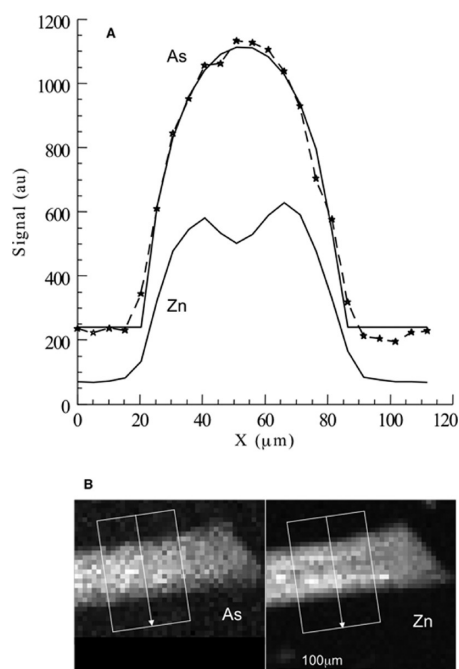
Figure 6. X-ray fluorescence emission signal for (A) transverse profiles of As (upper) and Zn (lower) in hair segment 3 and (B) microfocused X-ray fluorescence maps of As and Zn from which the lineouts in (A) were extracted. In (A) the upper curve, the dashed line with symbols represents the data while the solid line is the fit to eq 2 (see section 3.2 of the Supporting Information). The lower curve represents the data for Zn along the same transect as for As. In (B), the arrows show the transect plotted, and the width of the rectangles show the transverse width over which pixel values were averaged in order to reduce noise.

the mummy after S (Figure 4C, G, K, O, and S) and As (external contaminant) (Figure 4B, F, J, N, and R and Figure 6], shows a very different profile with uneven distribution and higher concentration in the outer part of the hair.

Arsenic K-edge μXANES revealed the presence of trivalent and pentavalent arsenic (Figure 7A). Arsenic species, both As(III) and As(V), were largely in the form of inorganic arsenic and to a lesser extent as organo-arsenic compounds. The predominant species identified in the hair samples was As(III) bound to S, either as As_2S_3 or AsCysteine with 27 ± 5% $As(V)O_4^{3-}$, although inorganic arsenic in surface and groundwater sources is mainly composed of arsenate ($As(V)O_4^{3-}$).[5] These findings are closely correlated with data from published arsenic speciation analyses in human hair from modern epidemiological studies in the Atacama Desert.[5] In consideration that the chronic arsenic poisoning is through ingestion of arsenic-contaminated drinking water, the higher amounts of As(III) species detected in the hair may be associated with the inclusion processes (biotransformation) of arsenic in the hair and the bioavailability of arsenic in the water.[5,26] However, time of exposure and age of the individuals as well as additional quantities of As(III) contained in vegetables and other edible plants consumed may have contributed to the assimilation of a higher arsenite level.[5]

Further comparison with studies on modern populations in rural areas of the Atacama Desert suggest that the presence of As(III) in the hair can be regarded as a good indicator for chronic arsenic exposure through the consumption of contaminated superficial and groundwater.[5,11] The Atacama Desert and the surrounding region of northern Chile is an
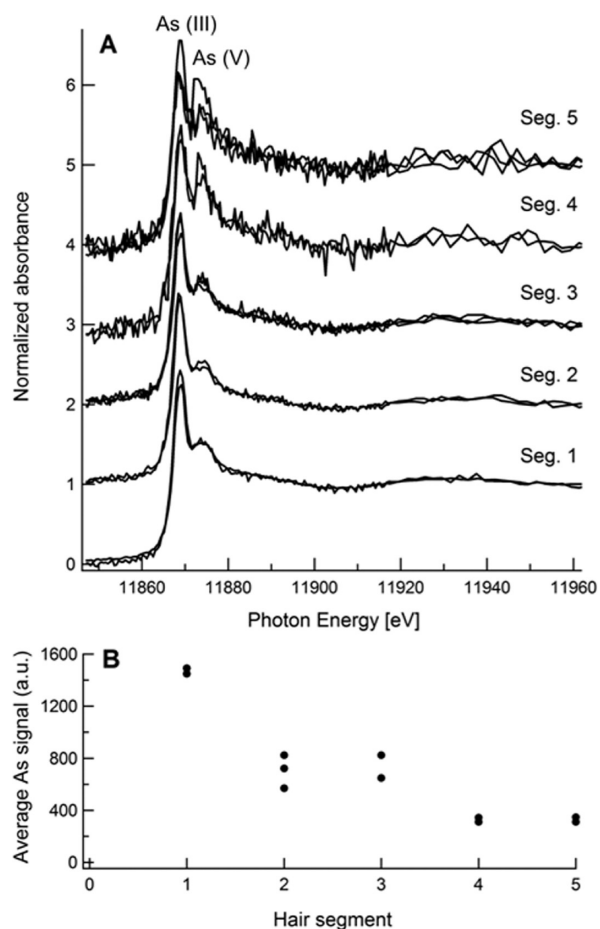

Figure 7. (A) Average As K-edge μXANES spectra collected from various spots on 5 hair segments along the entire hair shaft from the proximal (seg. 1) to the distal end (seg. 5). As (III) and As (V) are present in all hair segments analyzed. (B) Average arsenic counts on each segment, showing an almost 4× decrease in arsenic content in the distal end (tip) of the hair.

arsenic-rich geo-environment. We considered that the arsenic contained in tertiary-quaternary sediments, soils, and arsenic-containing metallic sulfides in the Andean highlands is leached out through geochemical processes and transported into regional rivers in the mid valleys of the Atacama Desert used as a drinking water source and to irrigate edible plants. Even today, while arsenic is removed from the water supply of major cities in Chile, rural areas in the Atacama Desert are still exposed to arsenic polluted drinking water sources.[5,11,27,28] The consumption of arsenic-contaminated water is the most common and major cause of arsenicism.[5] Despite the overall limited bioavailability of arsenic through drinking water, the chronic consumption can cause severe health effects to the exposed population, often accompanied by skin manifestations such as those observed on some of the mummies investigated here (Figure S1 of the Supporting Information).[1,15,27] The distribution and chemical speciation of arsenic along the hair shaft further supports biogenic incorporation, induced mainly by ingestion of arsenic-contaminated water.[8−12,14,15,29]

Quantitative measurements of the arsenic concentration within the different hair segments have further indicated a decrease of arsenic concentration toward the distal end (Figure 7B). This may indicate (1) depletion of arsenic due to chemical

and/or microbiological processes both in life and post-mortem[30] or (2) a change in the diet due to mobility.[10,31]

CONCLUSIONS

The characterization of the longitudinal and transverse profiles of arsenic in the hair and its oxidation state was essential to identify the origin and toxicity of this poisonous metalloid, reflecting a retrospective time span along the hair growth.[4,21] These data helped to discriminate from exogenous contamination induced by metallophillic bacteria as well as environmental heavy metal pollutant diffusion mechanisms based on physical contact during burial, as (1) the arsenic concentration in the burial enveloping soil does not exceed 30 ppm, a concentration consistent with uncontaminated sandy soils[32] and (2) the mummy investigated was wrapped in a bundle and not in direct contact with soil. Our data support a previous hypothesis of the existence of a native population circa AD 500−1450 in the Tarapacá Valley that has been adapted to local geopolitical, social, and economic conditions[33] and who lived and moved along the mid river valleys. This hypothesis is also supported by the observed reduction in the arsenic concentration from the proximal to the distal end of the hair that could be due to a change in diet due to mobility, though chemical and/or microbiologically induced processes cannot be entirely ruled out. The protocol for the scientific method used in this study,[34] demonstrating high sensitivity and high specificity in toxicity assessment and geographic mobility, was central to overcoming analytical challenges[20] and can be broadly applied to forensic investigations and environmental monitoring programs for which heavy metal quantification and sourcing is necessary.

ASSOCIATED CONTENT

S **Supporting Information**

Further content on materials and methods, sample preparation, hair geometry, and element concentration profiles used to support hypotheses made in this study. One additional experimental figure connected to analytical and characterization data (also referenced in the article). This material is available free of charge via the Internet at http://pubs.acs.org.

AUTHOR INFORMATION

Corresponding Author

*E-mail: kakoulli@ucla.edu.

Author Contributions

The manuscript was written through contributions of all authors. All authors have given approval to the final version of the manuscript. All authors contributed equally.

Notes

The authors declare no competing financial interest.

ACKNOWLEDGMENTS

REFERENCES

(1) Xia, Y. J.; Wade, T. J.; Wu, K. G.; Li, Y. H.; Ning, Z. X.; Le, X. C.; He, X. Z.; Chen, B. F.; Feng, Y.; Mumford, J. L. *Int. J. Environ. Res. Public Health* **2009**, *6* (3), 1010−1025.

(2) Chevallier, P.; Ricordel, I.; Meyer, G. *X-Ray Spectrom.* **2006**, *35*, 125−130. Nicolis, I.; Curis, E.; Deschamps, P.; Benazeth, S. *Biochimie* **2009**, *91*, 1260−1267.

(3) Wilson, A. S. In *Hair in Toxicology: An Important Biomonitor*; Tobin, D. J., Ed.; Royal Society of Chemistry: Cambridge, 2005; pp 321−345.

(4) Kempson, I. M.; Henry, D. A. *Angew. Chem., Int. Ed.* **2010**, *49*, 4237−4240.

(5) Yañez, J.; Fierro, V.; Mansilla, H.; Figueroa, L.; Cornejo, L.; Barnes, R. M. *J. Environ. Monit.* **2005**, *7*, 1335−1341.

(6) Paswan, S. *Studying the arsenic absorption by keratin protein extracted from human hair*. Bachelor of Technology Thesis, National Institute of Technology Rourkela, 2012.

(7) Allison, M. J. In *Human Mummies*; Spindler, K., Ed.; Springer-Verlag/Wien: New York, 1996; pp 125−129.

(8) Allison, M. J. Chronic arsenic poisoning in South American Mummies. *Annual Meeting of the International Academy of Pathology*, Washington D.C., March 1996.

(9) Arriaza, B.; Amarasiriwardena, D.; Cornejo, L.; Standen, V.; Byrne, S.; Bartkus, L.; Bandak, B. *J. Archaeol. Sci.* **2010**, *37*, 1274−1278.

(10) Byrne, S.; Amarasiriwardena, D.; Bandak, B.; Bartkus, L.; Kane, J.; Jones, J.; Yañez, J.; Arriaza, B.; Cornejo, L. *Microchem. J.* **2010**, *94*, 28−35.

(11) Figueroa, L. *Arica Inserta en una Región Arsenical: El Arsénico en Ambiente que la Afecta y 45 Siglos de Arsenicismo Crónico*; Universidad de Tarapacá: Arica, Chile, 2001. Figueroa, L.; Bazmilic, B.; Allison, M.; Gonzáles, M. *Chungará* **1988**, *21*, 33−42.

(12) Arriaza, B. T. *Chungará, Revista de Antropología Chilena* **2005**, *37*, 255−260.

(13) Leybourne, M. I.; Cameron, E. M. *Chem. Geol.* **2008**, *247*, 208−228.

(14) Pringle, H. *Science* **2009**, *324*, 1130−1130.

(15) Rahman, M.; Ng, J.; Naidu, R. *Environ. Geochem. Health* **2009**, *31*, 189−200.

(16) Kempson, I. M.; Henry, D.; Francis, J. *J. Synchrotron. Radiat.* **2009**, *16*, 422−427.

(17) Wilson, A. S.; Dodson, H. I.; Janaway, R. C.; Pollard, A. M.; Tobin, D. J. *Archaeometry* **2010**, *52*, 467−481. Bianucci, R.; Jeziorska, M.; Lallo, R.; Mattutino, G.; Massimelli, M.; Phillips, G.; Appenzeller, O. *PLoS ONE* **2008**, *3*, e2053. Phillips, G.; Reith, F.; Qualls, C.; Ali, A.-M.; Spilde, M.; Appenzeller, O. *PLoS ONE* **2010**, *5*, e9335.

(18) Kintz, P.; Ginet, M.; Cirimele, V. *J. Anal. Toxicol.* **2006**, *30*, 621−623. Kintz, P.; Ginet, M.; Marques, N.; Cirimele, V. *Forensic Sci. Int.* **2007**, *170*, 204−206.

(19) Forshufvud, S.; Smith, H.; Wassen, A. *Nature* **1961**, *192*, 103−105. Kintz, P.; Goulle, J. P.; Fornes, P.; Ludes, B. *J. Anal. Toxicol.* **2002**, *26*, 584−585.

(20) Pezzotti, G.; Sakakura, S. *J. Biomed. Mater. Res.* **2003**, *A*, 230−236.

(21) Wilson, A. In *Soil Analysis in Forensic Taphonomy: Chemical and Biological Effects of Buried Human Remains*, Tibbett, M.; Carter, D. O., Eds.; Taylor & Francis Group: Boca Raton, FL, 2008.

(22) Wilson, A. S.; Dodson, H. I.; Janaway, R.; Pollard, A.; Tobin, D. *Br. J. Dermatol.* **2007**, *157*, 450−457.

(23) Lubec, G.; Zimmerman, M. R.; Teschler-Nicola, M.; Stocch, V.; Aufderheide, A. C. *Free Radical Res.* **1997**, *26*, 457−462.

(24) Berger, I. A.; Cooke, R. U. *Earth Surf. Processes Landforms* **1997**, *22*, 581−600. Clarke, J. D. A. *Geomorphology* **2006**, *73*, 101−114. Duncan, P. B.; Morrison, R. D.; Vavricka, E. *Environ. Forensics* **2005**, *6*, 205−215. Katz, H. R. *Miner. Deposita* **1967**, *2*, 131−134. Kholodov, V. N. *Lithol. Miner. Resour.* **2007**, *42*, 246−256. Rech, J. A.; Currie, B. S.; Shullenberger, E. D.; Dunagan, S. P.; Jordan, T. E.; Blanco, N.; Tomlinson, A. J.; Rowe, H. D.; Houston, J. *Earth Planet. Sci. Lett.* **2010**, *292*, 371−382.

(25) Smith, H. *J. Forensic Sci. Soc.* **1964**, *4*, 192−199.

(26) Steely, S.; Amarasiriwardena, D.; Jones, J.; Yañez, J. *Microchem. J.* **2007**, *86*, 235−240.

(27) Smith, A. H.; Arroyo, A. P.; Mazumder, D. N. G.; Kosnett, M. J.; Hernández, A. L.; Beeris, M.; Smith, M. M.; Moore, L. E. *Environ. Health Perspect.* **2000**, *108*, 617−620.

(28) Smith, A. H.; Lopipero, P. A.; Bates, M. N.; Steinmaus, C. M. *Science* **2002**, *296*, 2145−2146.

(29) Smith, E.; Kempson, I; Juhasz, A. L.; Weber, J.; Skinner, W. M.; Grafe, M. *Chemosphere* **2009**, *76*, 529−535.

(30) Muller, D.; Médigue, C.; Koechler, S.; Barbe, V.; Barakat, M.; Talla, E.; Bonnefoy, V.; Krin, E.; Arsène-Ploetze, F.; Carapito, C. *PLoS Genetics 3* **2007**, e53. Hindmarsh, J. T. *Clinical Biochemistry* **2002**, *35*, 1−11.

(31) Knudson, K. J.; Price, T. D. *Am. J. Phys. Anthropol.* **2007**, *132*, 25−39. Sturgis, R. The Macmillan Company: New York, 1905, 2.

(32) Mandal, B. K.; Suzuki, K. T. *Talanta* **2002**, *58*, 201−235.

(33) Uribe, R. M. In *Esferas de Interacción Prehistóricas Y Fronteras Nacionales Modernas: Los Andes Sur Centrales*; Lechtman, H., Ed.; Instituto de Estudios Peruanos, Lima (IEP) and the Institute of Andean Research, New York (IAR): Lima and New York, 2006.

(34) Kempson, I. M.; Kirkbride, K. P.; Skinner, W. M.; Coumbaros, J. *Talanta* **2005**, *67*, 286−303. Martin, R. R.; Kempson, I. M.; Naftel, S. J.; Skinner, W. M. *Chemosphere* **2005**, *58*, 1385−1390.